Field Distribution and Dispersion Characteristics of Fundamental and Higher-Order Modes in Miniature Hybrid MIC (MHMIC) Considering Finite Conductor Thickness and Conductivity

Ke Wu and Ruediger Vahldieck

Laboratory for Lightwave Electronics, Microwaves and Communications
(LLiMiC)
Department of Electrical and Computer Engineering, University of Victoria
Victoria, B.C., V8W 3P6, Canada

Abstract

A hybrid-mode analysis of coplanar transmission lines on 10mils alumina substrate with lossy back metallization is presented. A self-consistent approach is used together with the method of lines (MoL) to determine the propagation constant, losses and field distribution considering finite metallization thickness and conductor losses. Results are given for the fundamental and first two higher-order modes. It is demonstrated that the onset of higher order modes limits the frequency range of conductor backed CPW's.The method presented is general and can be used in the analysis of Miniature Hybrid MIC's (MHMIC) and MMIC's and can include also semiconductor losses.

Introduction

Considering conductor losses becomes extremely important in the design of Miniature Hybrid MIC's and MMIC's. A great number of researchers worldwide has dealt with this problem in detail (i.e. [1]-[5]) but very little information is available on conductor backed CPW's (or slotlines) on thin (<10 mils) allumina or GaAs substrate nor is there any information about the influence of the different types of losses and backmetallization on the first higher-order modes. Although uniplanar structures are most attractive, be it for MHMIC's or for MMIC's, the shielding metallization of the final chip or the mounting jig is usually not far away from the top plane of the uniplanar circuit and can thus cause a change in the propagation characteristic which, if uncontrolled, can alter the circuit performance in an unexpected way. Therefore, not only is it necessary to include the back metallization into the general analysis but it is also necessary to consider its losses due to finite conductivity. The latter point is in particular of interest in the case of microstrip lines.
To address these problems, this paper presents a theoretical analysis of propagation properties of conductor-backed CPW transmission lines on 10mils alumina substrate. Of particular concern is the effect of conductor losses on the first two higher order modes and how the field configuration changes under the influence of conductor losses. To verify the results, measurements will be presented.

Commonly used perturbation methods or Wheeler's incremental inductance rule are clearly not suitable for this task since the miniaturized dimensions of the transmission lines are frequently in the order of or even smaller than the skin depth. Also, due to the thin substrate thickness and the close vicinity of the back metallization to the center conductor, quasi-TEM mode propagation is not likely at higher frequencies. Therefore, it is important to use a full wave analysis to accurately determine the frequency limitations and propagation characteristics of uniplanar structures, in particular CPW's or slotlines, in the presents of conductor losses.

Among the different methods that have been developed in the past, the self consistent description of metallic losses, which describes the metallic layer as lossy dielectric, together with the mode matching method [2] were most promising. For example, this research had shown that, under certain conditions and contrary to the traditional perception the propagation constant in a CPW at low frequencies shows a negative slope if conductor losses are considered. These theoretical results have been confirmed recently in an experiment [5].
Since the mode matching method is known for its relative convergence behaviour and its limitations in terms of rectangular circuit contours, we have adopted the self consistent approach for the MoL [3] at approximately the same time as the authors in [4]. However, the analysis presented here goes beyond the presentation in [3] and [4] and includes also higher-order modes in the analysis. Although the analysis is most general and can be applied to slotlines and microstrip lines on lossless as well as lossy semiconductor substrate, the present investigation is limited to CPW's only.

Theory

In the self-consistent approach the lossy conductor area is treated as an ordinary lossy dielectric region which is characterized by its complex dielectric permittivity. The imaginary part of this complex value is usually very high because it represents the conductivity of the material used.
Based on this assumption the transmission line cross-section can be regarded as multilayered dielectric structure with inhomogeneous subregions. The first layer represents the different conductor regions. The groundplane is an imperfect conductor on the backside of the supporting (Alumina) substrate material, but usually thicker than the strips on the substrate surface, therefore a skin-effect layer is assumed on this groundplane as an additional layer with finite conductivity σ_g. The thickness of this layer equals the skin depth

$$t_4 = \delta = \sqrt{\frac{2}{\omega\mu_o\sigma_g}} \quad \ldots\ldots \qquad (1)$$

CH2870-4/91/0000-0995$01.00 © 1991 IEEE

Within the inhomogeneous layer the dielectric permittivity $\varepsilon_r(x)$ changes abruptly. Therefore, the electromagnetic field for each electric and magnetic discretization line is expressed as a superposition of LSM/LSE potentials functions rather than TE/TM potential functions:

$$\vec{E} = \frac{1}{j\omega\varepsilon_o\varepsilon_r(x)}\nabla\times\nabla\times\left(\Psi^e\vec{e}_x\right) - \nabla\times\left(\Psi^h\vec{e}_x\right)$$

$$\vec{H} = \nabla\times\left(\Psi^e\vec{e}_x\right) + \frac{1}{j\omega\mu_o}\nabla\times\nabla\times\left(\Psi^h\vec{e}_x\right) \tag{2}$$

The scalar functions Ψ^e and Ψ^h must satisfy the Helmholtz and Sturm-Liouville equations, respectively:

$$\frac{\partial^2\Psi^h}{\partial y^e} + \frac{\partial^2\Psi^h}{\partial x^e} + \left(\varepsilon_r(x)k_o^z - \beta^z\right)\Psi^h = 0$$

$$\frac{\partial^2\Psi^e}{\partial y^z} + \varepsilon_r(x)\frac{\partial}{\partial x}\left(\frac{1}{\varepsilon_r(x)}\frac{\partial\Psi^e}{\partial x}\right) + \left(\varepsilon_r(x)k_o^z - \beta^z\right)\Psi^e = 0 \tag{3}$$

After discretizing the x-variable and decoupling the spatially coupled discretization lines [4] one obtains a decoupled ordinary differential equation for the e-lines (and similar for h-lines)

$$\frac{d^2\tilde{v}^e}{dy^2} - \left[\overbrace{\left(\frac{[\tilde{\varepsilon}^e][\delta][\tilde{\varepsilon}^h]^{-1}[\delta]^t}{h_o^2} - [\tilde{\varepsilon}^e]k_o^2\right)}^{\bar{k}^{e^2}}\beta^e + \beta^2\right]\tilde{v}^e = 0 \tag{4}$$

which corresponds to simple wave equations. Furthermore, utilizing the interface condition between homogeneous subregions one can derive a Green's matrix in the transformed domain which becomes a space domain Green's function after the inverse transformation [7]

$$\begin{pmatrix}\tilde{Y}_{xx} & \tilde{Y}_{xz}\\ \tilde{Y}_{zx} & \tilde{Y}_{zz}\end{pmatrix}\begin{pmatrix}j\vec{E}_x\\ \vec{E}_z\end{pmatrix} = 0 = \begin{pmatrix}\vec{I}_x\\ j\vec{I}_z\end{pmatrix} \tag{5}$$

Equation (5) must now be solved for the zero's of the matrix **Y** to find the complex propagation constant.

Results

The structure under investigation is shown in Fig.1 together with measurements of the return loss, which show clearly the onset of a higher-order mode at about 25GHz. The calculated dispersion diagram including losses for the fundamental and two first higher-order modes are shown in Fig.2. It is interesting to see that at about 23-25GHz two higher-order modes start to propagate which confirms the measurements. Due to these higher-order modes a substantial amount of power normally carried by the fundamental mode is now converted into a higher-order mode and causes a high return loss. Another interesting observation from Fig.2 is that the fundamental mode propagation constant shows a negative slope versus frequency. This tendency is in particularily obvious at lower frequencies up to 0.5GHz. Such a behaviour is similar to that of a slow-wave mode and can be explained in a similar fashion.

Fig.3 displays the real part of the Ex-field component for different modes directly in the interface plane between the conductor plane and the dielectric at different frequencies. It should be mentioned that because of the small center conductor a non-equidistant discretization has been used. It is obvious from the figure that at 15GHz the fundamental mode behaves as expected, showing a high field magnitude at the edges of the conductor and the uniplanar groundplane. It is also shown in Fig.3 that at 32 GHz and at the edge of the uniplanar groundplane this Ex-field is zero, which indicates that the fundamental mode is not any longer concentrated in the slot area. At the same frequency the Ex-field of the first two higher-order modes are increased, indicating that they carry more power in the slot area, which was not the case below their cutoff frequency. The field orientation of this second higher order mode is clearly incompatible with the field required in the coax launcher and therefore must also lead to high reflection losses. Fig.4 illustrates the Ex-field in a plane half the substrate thickness below the conductor plane. The Ey-field is shown in Fig.5 at the same location as the Ex-field in Fig.4. It is obvious that even at 15 GHz there is already a relatively strong Ey-field concentration below the center conductor which increase at 32 GHz as expected. The field distribution cannot be clearly assigned to the TEM or one of the known TE or TM modes. Therefore, the modes that propagate on that line are of hybrid nature and even at lower frequencies (15GHz) the quasi-TEM mode cannot be described as even or odd mode but rather a combination of both.

Conclusion

This paper has presented a theoretical analysis of propagation characteristics in conductor-backed CPW transmission lines on 10 mils alumina substrate. It was found that the thin substrate allows higher order modes to propagate at frequencies lower than 30GHz. Under the influence of conductor losses the field distribution for the fundamental mode becomes hybrid even at lower frequencies and at very low frequencies (<1GHz), there is a negative slope of the propagation constant versus frequency.

Acknowledgement

The authors would like thank Dr. J. Fikart and H. Minkus from MPR Teltech Ltd, Vancouver for helpful discussions and fabrication of the MHMIC circuit samples. This work was jointly funded by MPR Teltech Ltd and the National Science and Engineering Research Council of Canada (NSERC) under the Cooperative Research and Development (CRD) program.

References

[1] Finlay, H.J., R.H. Jansen, J.A. Jenkins and I.G. Eddison,"Accurate Characterization and Modelling of Transmission Lines for GaAs MMIC's", IEEE Trans. Microwave Theory and Tech., vol.36, pp.961-967, June 1988.

[2] Heinrich, W.,"Full-Wave Analysis of Conductor Losses on MMIC Transmission Lines," IEEE Trans. Microwave Theory and Tech., vol.38, pp.1468-1472, Oct. 1990.

[3] Wu, K. and R. Vahldieck,"A Self-Consistent Approach to Dteremine Loss Properties in MIC/MMIC Coplanar Transmission Lines," in Proceedings of the 3rd Asia-Pacific Microwave Conference , Sept.18-21, 1990, Tokyo, Japan,pape 35-4, pp.823-826.

[4] Schmückle, F.J. and R. Pregla,"The Method of Lines for The Analysis of Lossy Waveguides," IEEE Trans. Microwave Theory and Tech., vol.38, pp.1473-1479, Oct.1990.

[5] Shih, Y.-C. and M. Maher," Characterization of Conductor-Backed Coplanar Waveguides Using Accurate On-Wafer Measurement Techniques," in Intl. IEEE Microwave Symposium Digest, Dallas, pp 1129-1132, 1990.

[6] Hirota, T. Y. Tarusawa and H. Ogawa, "Uniplanar MMIC Hybrids - A proposed New MMIC Structure," IEEE Trans. Microwave Theory and Tech., vol.35, pp.576-581, June 1987.

[7] Diestel, H., and S. B. Worm, "Analysis of hybrid field problems by the method of lines with non-equidistant discretization", IEEE Trans. Microwave Theory and Tech., vol. MTT-32, pp. 633-638, June 1984.

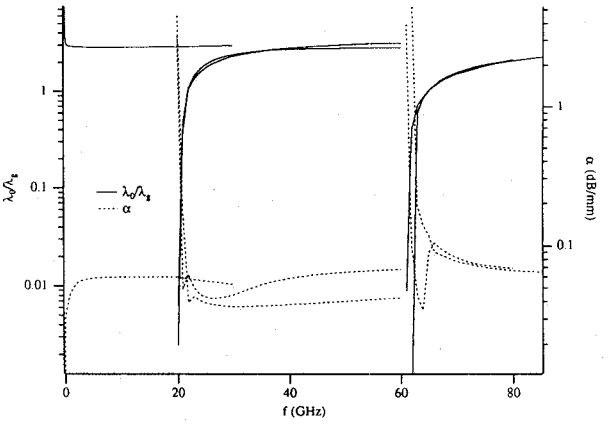

Fig.2

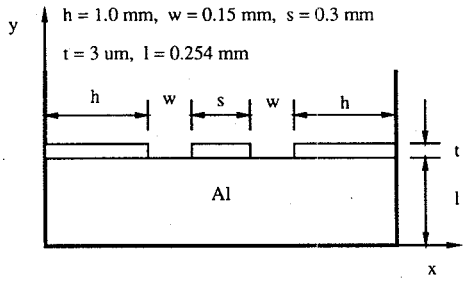

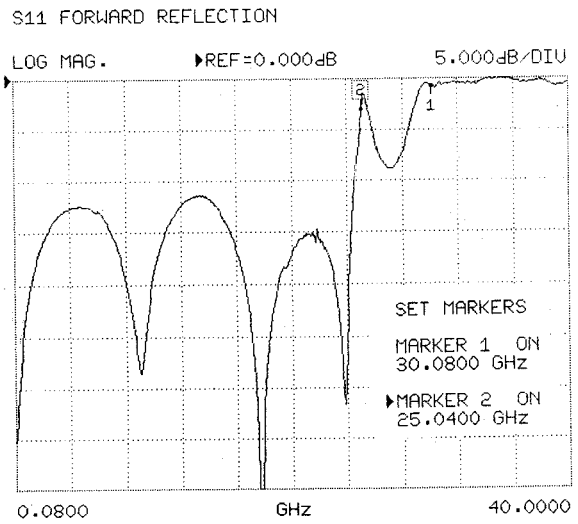

Fig.1

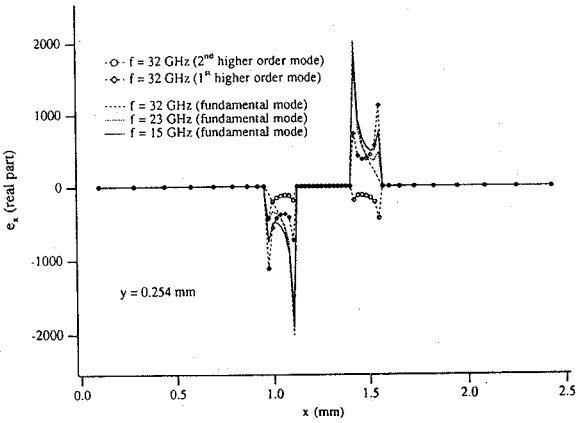

Fig.3

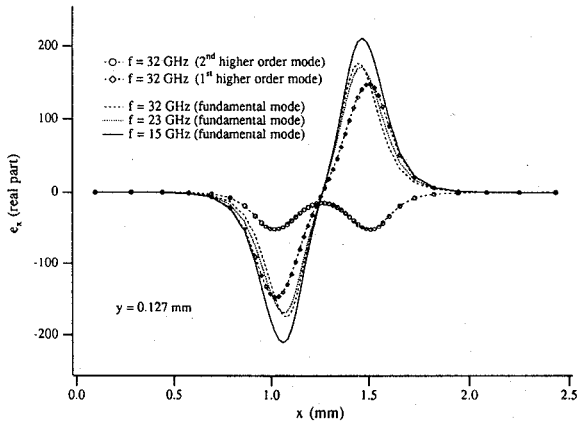

Fig.4

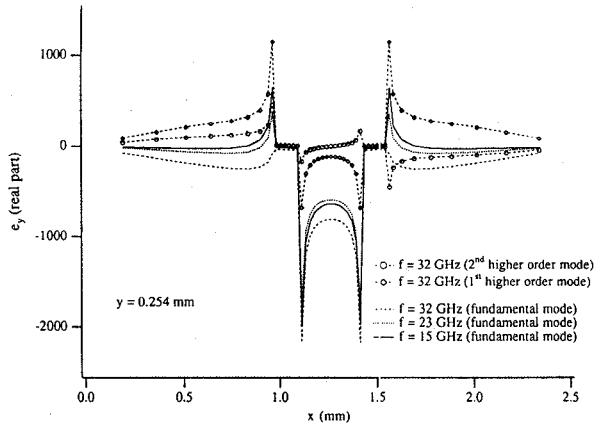
1000
0
-1000
-2000
e_y (real part)
y = 0.254 mm
f = 32 GHz (2nd higher order mode)
f = 32 GHz (1st higher order mode)
f = 32 GHz (fundamental mode)
f = 23 GHz (fundamental mode)
f = 15 GHz (fundamental mode)
0.0
0.5
1.0
1.5
2.0
2.5
x (mm)

Fig.5

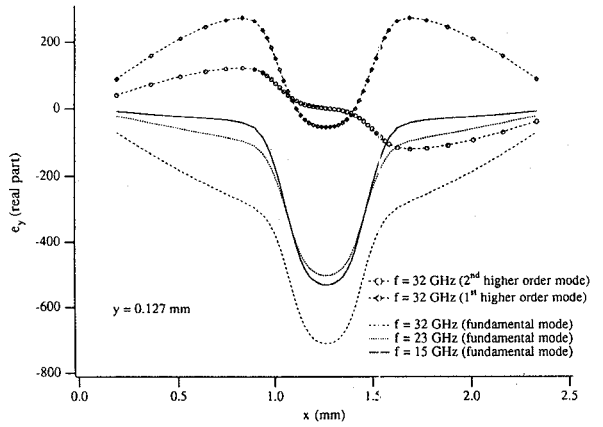
200
0
-200
-400
-600
-800
e_y (real part)
y = 0.127 mm
f = 32 GHz (2nd higher order mode)
f = 32 GHz (1st higher order mode)
f = 32 GHz (fundamental mode)
f = 23 GHz (fundamental mode)
f = 15 GHz (fundamental mode)
0.0
0.5
1.0
1.5
2.0
2.5
x (mm)

Fig.6